Ring-Coupled-Oscillator Sequentially Rotated Active Antenna

Suidong Yang, Vincent F. Fusco, *Senior Member, IEEE*, and Denver E. J. Humphrey, *Member, IEEE*

***Abstract*—In this paper, an active four-element patch antenna, backed by four GaAs monolithic-microwave integrated-circuit (MMIC) 4.4-GHz oscillators, self-locked by mutual coupling through a lumped capacitive ring MMIC network, has been designed, fabricated, and tested. The sequentially rotated arrangement given here when augmented with a lumped capacitive coupling network suggests that in-phase oscillator entrainment is guaranteed so that spatial power combination by the antenna array occurs with circular polarization characteristics.**

***Index Terms*—Antenna array, injection locking, microwave oscillators, MMIC, spatial power combining.**

I. Introduction

THE growth in the requirement for RF power sources at microwave frequencies for low-cost spatial power combining in personal communications and radar systems has been considerable [1]–[3]. Coupled active antenna oscillator arrays, which can be injection locked to form electronic beam-scanning arrays without phase shifters, have been realized in spatial power-combining technology at microwave and millimeter-wave spatial frequencies [4]–[7]. It is also known that coupled-oscillator modal stability can be improved by coupling the oscillators through lumped resistive or capacitive elements [8], [9]. A four-element four-coupled-oscillator-fed sequentially rotated circularly polarized array consisting of rectangular patch elements excited with amplifier enforced unidirectional feeding was presented in [10] and an earlier three-element variant was presented in [11]. The configuration to be discussed in this paper is much simpler to implement since it does not require additional RF circuitry to enforce unidirectional signal flow, as this is not a requisite for stable operation of the system proposed here.

In this paper, we show how a sequentially rotated patch antenna consisting of linearly polarized circular patch-antenna elements can be realized in order to produce in-phase microwave power combining at circuit and at spatial levels with circular polarization characteristics. The arrangement suggested should considerably reduce corporate feed requirements when the 2×2 antenna discussed here is used as a building block in a larger array.

Manuscript received November 23, 1999; revised January 18, 2001. This work was supported by the Engineering and Physical Sciences Research Council and by Marconi GEC under Contract GR/K58449.

S. Yang and V. F. Fusco are with the High Frequency Electronics Laboratory, Department of Electrical and Electronic Engineering, The Queen's University of Belfast, Belfast BT9 5AH, Northern Ireland (e-mail: v.fusco@ee.qub.ac.uk).

D. E. J. Humphrey was with the High Frequency Electronics Laboratory, Department of Electrical and Electronic Engineering, The Queen's University of Belfast, Belfast BT9 5AH, Northern Ireland. He is now with TDK Ireland, Belfast BT9 5QH, Ireland.

Publisher Item Identifier S 0018-9480(01)06136-1.

II. Ring Coupled-Oscillator Design and Simulation

Fig. 1(a) shows the monolithic-microwave integrated-cicuit (MMIC) oscillator designed to operate at 4.4 GHz and its electrical schematic circuit is given in Fig. 1(b). The oscillator was fabricated as a MMIC using the GEC-Marconi Materials Technology (GMMT) F20 process [12] and was designed to be biased from a single 1.2-V dc supply. As reported in [9], complete oscillator behavior can be approximated by a Van der Pol oscillator model [13]. In order to combine the outputs from the four oscillators together, a MMIC lumped-capacitive ring coupling network has been developed, which is shown in Fig. 1(c). Here, the coupling through the lumped capacitive network is designed to dominate the oscillator entrainment process, and ensure, at the center of the mutual locking range, in-phase power combining, as described later in this paper. The mutual coupling through free space between the antenna radiating elements in the array is also considered and is found to have only a second-order effect on oscillator frequency of operation when operated in the presence of the lumped capacitive coupling network.

The four separate MMIC feedback oscillators shown in Fig. 1(a), capacitive coupling network shown in Fig. 1(c), and antenna assembly shown in Fig. 2(b) were brought together into a larger module, as shown in Fig. 2(c). Here, the individual MMIC oscillators are coupled together using the 10-pF chip capacitive ring MMIC bonded using 2-mm-long gold wire of 25-μm diameter, and the bond-wire inductance was estimated to be approximately 0.2 nH.

Measured characteristics for the individual oscillators are presented in Table I. In total, 50 oscillator chips were tested, which resulted in the tolerance spreads cited in Table I.

To accommodate the spreads in power and frequency characteristics obtained within the batch tested, coefficients a and b required for (1) were extracted to accommodate a negative conductance $G(v)$, which would yield a nominal mean value of output power of 4.3 mW obtained for a dc voltage of 1.2 V, as shown in Table I. Simulated L, C values were chosen to match the oscillator resonant frequency, and these values were then used in the theory presented below.

The phase noise for the oscillator at this bias level was measured to be -40 dBc/Hz at 10 kHz from the carrier, and -66 dBc/Hz at 100 kHz, suggesting that the relatively low-Q factor of the oscillator, i.e., 2.6, makes it suitable for frequency entrainment by mutual coupling. All the harmonics in the output signal were seen to be down by at least -30 dB on the fundamental level.

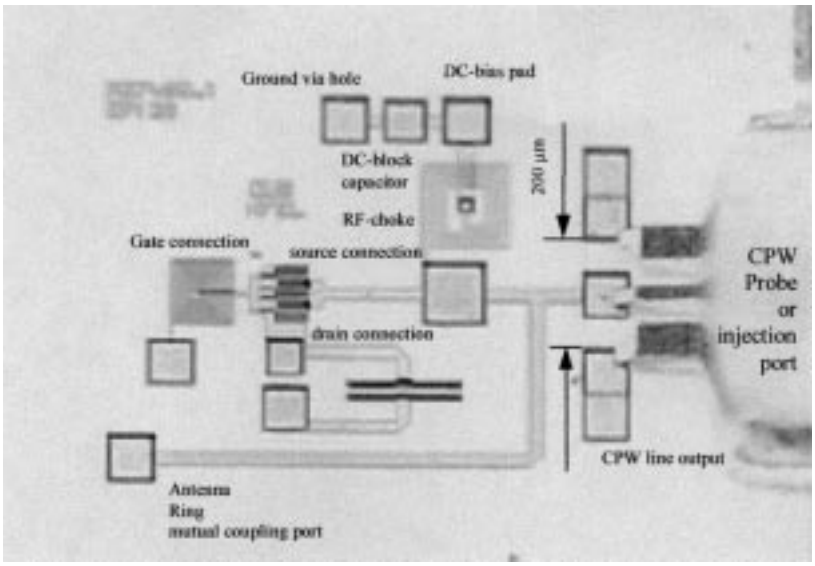

(a)

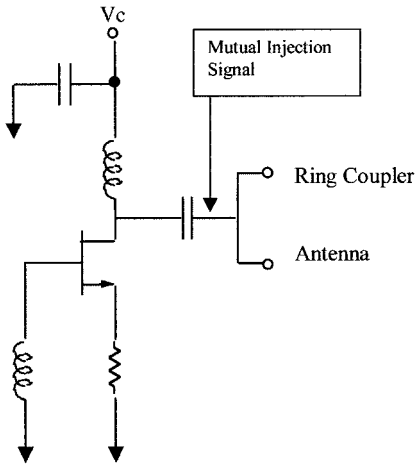

(b)

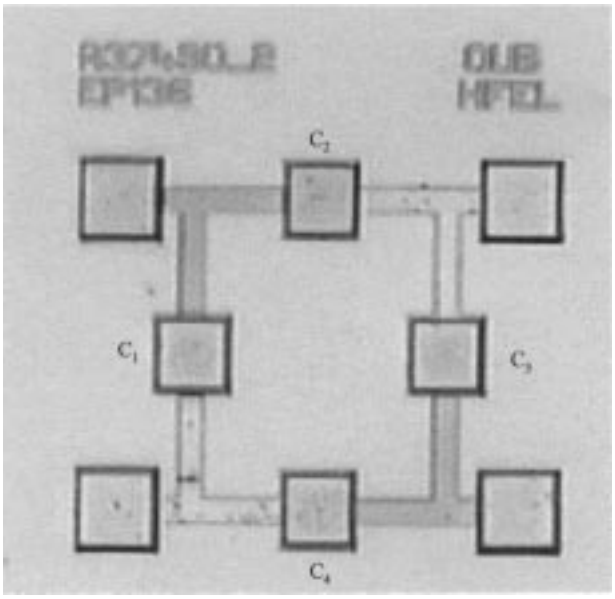

(c)

Fig. 1. Circuit components used in an active antenna element. (a) Self-biased 4.4-GHz oscillator. (b) Self-biased oscillator schematic. (c) Capacitive coupling MMIC ring network layout. $C_1 = C_2 = C_3 = C_4 = 10$ pF.

III. Coupling Theory

The nonlinear conductance for each oscillator representing each active device [4] is

$$G(V) = \frac{i}{V} = -a + bV^2 \tag{1}$$

where V is the oscillator output voltage across the load and i is the nonlinear current coming from the device. Coefficients a and b are positive constants, evaluated by fitting the simulated current flowing into the load port of a single isolated nonlinear SPICE oscillator model as a function of the magnitude of a virtual voltage source connected at this port with the load removed [4]. For our device, the nominal values of a and b are $a = 2.32 \times 10^{-2}$ and $b = 3.82 \times 10^{-2}$. The required value for the Van der Pol model capacitance C (5.45 pF) and inductance L (0.24 nH) are estimated from a full nonlinear simulation of the oscillator behavior including the load impedance presented by the antenna (this aspect is described in more detail later in this section).

The characteristic equation of the coupled-oscillator array in Fig. 2(a) can be analyzed using Kirchoff's laws to form a Van der Pol equation [9], which can be used to describe the characteristic dynamical behavior of the capacitively coupled-oscillator ring

$$I_{\text{inj}} = i + C\frac{dV}{dt} + \frac{1}{L}\int V dt + \frac{V}{R_L} \tag{2}$$

where I_{inj} represents the injected current due to the lumped and mutual coupling networks. Equation (2) is rearranged to form

$$\frac{dV}{dt} + \omega_o^2 \int V dt + \frac{\omega_o V}{Q}\left[1 + R_L\left(-a + bA^2\right)\right] = \frac{I_{\text{inj}}}{C} \tag{3}$$

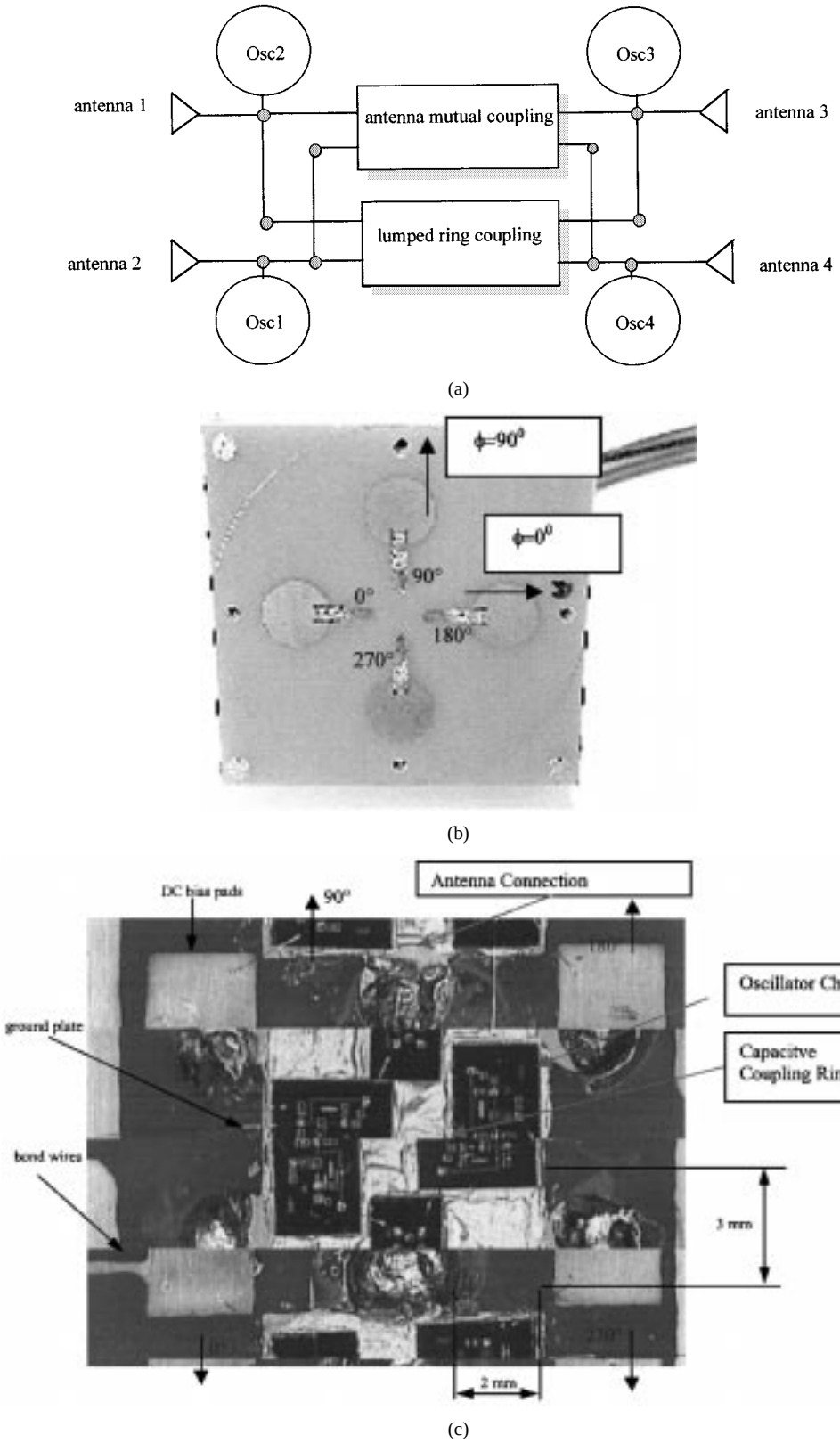

Fig. 2. Active ring oscillator configuration. (a) Schematic. (b) Top. (c) Bottom.

where

$$V = Ae^{j(\omega_L t+\varphi)} \tag{4}$$

$$\omega_o^2 = \frac{1}{LC} \tag{5}$$

$$Q = \omega_o R_L C. \tag{6}$$

By inserting (4)–(6) into (3) and following the solution procedure in [3] after equating real and imaginary parts for the kth oscillator, the decoupled equations for the amplitude and phase

TABLE I
DC PUSHING CHARACTERISTICS

Vdc (V)	0.8	1.0	1.2	1.4	1.6	1.8	2.0
P (dBm)	-13±0.5	0.7±0.1	4.3±0.1	6.7±0.1	8.1±0.2	8.9±0.2	9.5±0.2
f (GHz)	4.411 ±0.018	4.413 ±0.015	4.418 ±0.017	4.423 ±0.019	4.427 ±0.021	4.429 ±0.021	4.431 ±0.023
Idc (mA)	19±1	21±1	22±1	23±1	24±1	25±1	26±1
Q_{OSC}	2.2	2.5	2.6	3.4	4.6	6.7	8.8

dynamics are formed for the ring-coupled-oscillator configuration

$$\frac{dA_k}{dt} + \frac{\omega_k}{2Q_k} A_k\left[1 + R_{Lk}\left(-a_k + b_k A_k^2\right)\right] = \frac{I_{R\text{inj}k}}{2C_k} \tag{7}$$

$$\frac{d\varphi_k}{dt} + \omega_L - \omega_k = \frac{I_{I\text{inj}k}}{2A_k C_k} \tag{8}$$

where $I_{R\text{inj}k}$ and $I_{I\text{inj}k}$ are the real and imaginary components of the injection current, respectively, Q_k is the oscillator Q factor, C_k is the Van der Pol capacitance, R_{Lk} is the kth oscillator load, ω_L is the injection-locked frequency, and ω_k is the free-running kth oscillator frequency. External injection locking is permitted at the load (R_{Lk}) of each oscillator. Other injection-locking currents are provided by the unsynchronized oscillator induced currents flowing through the lumped coupling impedances and/or by the phase-delayed mutual coupling between array elements. Therefore, the lumped coupling element is written in terms of real and imaginary components (assumed to have the form of a conductance G_{kl} and a susceptance B_{kl}), while the inter-element mutual coupling, as described by York and Compton [14], is expressed in terms of magnitude and phase. Under these conditions, (7) and (8) are rewritten as

$$\begin{aligned}\frac{dA_k}{dt} &+ \frac{\omega_k}{2Q_k} A_k\left[1 + R_{Lk}\left(-a_k + b_k A_k^2\right)\right] \\ &= \frac{1}{2C_k}\left[D_k\cos(\theta_k - \varphi_k) + \sum_{\substack{l=1\\ l\neq k}}^{N} A_l \right. \\ &\qquad \left. \cdot \begin{bmatrix} G_{kl}\cos(\varphi_l - \varphi_k) - B_{kl}\sin,(\varphi_l - \varphi_k) \\ -A_k G_{kl} + \lambda_{lk}\cos(\varphi_l - \varphi_k - \psi_{lk}) \end{bmatrix}\right]\end{aligned} \tag{9}$$

$$\begin{aligned}\frac{d\varphi_k}{dt} &+ \omega_L - \omega_k \\ &= \frac{1}{2A_k C_k}\left[D_k\sin(\theta_k - \varphi_k) + \sum_{\substack{l=1\\ l\neq k}}^{N} A_l \right. \\ &\qquad \left. \cdot \begin{bmatrix} G_{kl}\sin(\varphi_l - \varphi_k) + B_{kl}\cos(\varphi_l - \varphi_k) \\ -A_k B_{kl} + \lambda_{lk}\sin(\varphi_l - \varphi_k + \psi_{lk}) \end{bmatrix}\right]\end{aligned} \tag{10}$$

where $D_k e^{j(\omega_L t + \theta_k)}$ represents the injection-locking signal from an external source to the kth oscillator and its effect on the whole array can be evaluated if required.

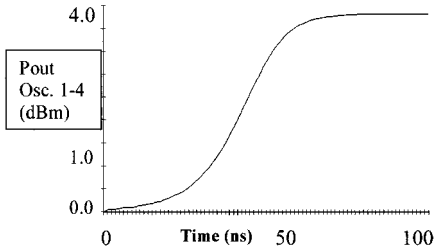

Fig. 3. Time-domain simulation results for ring oscillator.

The steady-state output behavior of the system occurs when

$$\frac{dA_k}{dt} = 0 \tag{11}$$

and

$$\frac{d\varphi_k}{dt} = 0. \tag{12}$$

From these equations, the steady-state entrained frequency ω_L, the individual peak amplitudes A_k, and the relative phases with respect to the first oscillator ϕ_k can be calculated by least-squares optimization. Numerical simulation of (11) and (12) show that frequency entrainment of the four capacitively coupled oscillators forming the oscillator ring can be obtained. Consequently, this implies that in-phase power combining via this approach is a possibility.

From comprehensive simulations, it was found that, when the lumped ring capacitance was below 1 pF, the oscillators do not phase lock to each other, while for $C_{\text{ring}} = 10$ pF, they run in phase with identical amplitudes. For simulation purposes, 0.2-nH bond wire inductances were included in series at each of the capacitor connection points, as shown in Fig. 2(c). Under locked conditions, the static phase-locking error between oscillators was observed by time-domain simulation [14] to be less than 10° when examined at times greater than 70 ns from switch on. Fig. 3 shows the overall transient amplitude response for the in-phase locked case ($C_{\text{ring}} = 10$ pF). Here, all oscillators are running with identical amplitude characteristics. Thus, the predicted dynamical behavior of this model suggests a dominant in-phase mode preference for identical or near-identical oscillators. This finding establishes the basic utility of the ring-coupled-oscillator configuration as a multiport power source in an in-phase power-combining array.

A time-domain analysis on HP MDS [15], which incorporates HP HFSS [16] derived free-space coupling between the antenna elements in the form of a Z matrix, derived from simulated port-to-port S-parameters, shows that the inclusion of free-space mutual coupling has a very minor effect on the mode formed in the presence of the capacitive ring elements. Its only

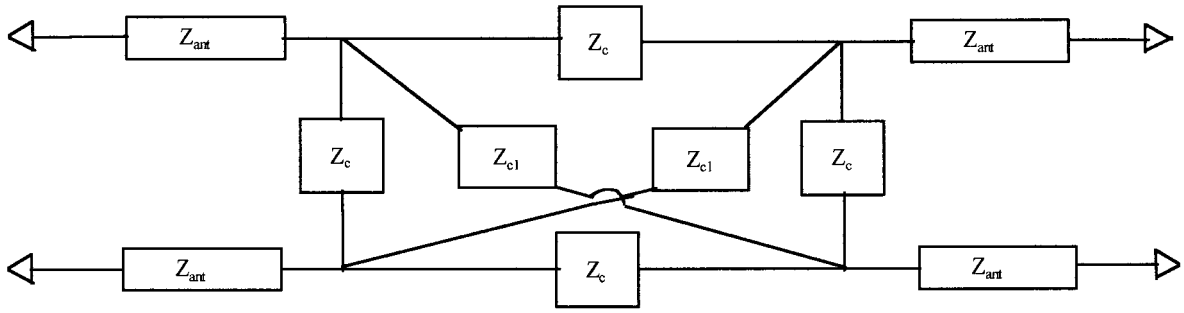

Fig. 4. Network model of array coupling ($Zant = 55 - j0.002\ \Omega$, $Zc = 10 + j2270\ \Omega$, $Zc1 = 1000 + j2270\ \Omega$).

effect appears to be the reduction of the entrained frequency of the locked system by a few megahertz. Further, its presence does not destabilize the dominant in-phase locked-oscillator mode established by the capacitive coupling network.

In order to employ HP MDS in this role, it is necessary that a circuit-based mutual-element-coupling model for the antenna structure proposed in the following section be established. Since the simulated mutual couplings through free space between any two of the circular radiating elements in Fig. 2(b) are symmetric, a simplified equivalent electrical circuit representing both the lumped and mutual coupling for the antenna array can be developed, as shown in Fig. 4. This circuit is used as the load for the lumped coupled ring oscillators shown in Fig. 2(a).

IV. Antenna Head Design

Each antenna (constructed on 1.6-mm $\varepsilon_r = 4.55$ printed circuit board) was chosen in order to facilitate symmetrical coupling to be a 4.4-GHz circular patch antenna operating at its fundamental mode, spaced by 0.8 λ_o, and matched using an inset microstrip feed to 50 Ω. The simulated return loss for each element of the active antenna array was better than -32 dB. Experimentally, a return loss of -16 dB at each antenna port was achieved at 4.4 GHz with a bandwidth of 250 MHz, the measured Q factor of the completed assembly is 18 and the simulated antenna gain is 5.6 dBi.

The structure of the antenna is shown in Fig. 2. Each antenna is connected to one of the outputs of the ring-coupled network with progressive 90° phase delays by adding line lengths to ensure required circular polarization action via sequential rotation [17]. Simulated far-field patterns predicts a bore-sight axial ratio 1.5 dB for the antenna (measured 2.8 dB) and 3-dB axial beamwidth in the principle planes 40° measured (45° simulated), diagonal planes 30° (40° simulated).

V. Active Ring System

Fig. 2(b) and (c) shows the constructional details of the oscillator assembly working at the 4.4-GHz locked frequency. This stable locked mode is seen to exist even when there is 0.5-dB power difference and 23-MHz oscillation frequency deviation, i.e., within the expected manufacturing spread of the individual oscillators, as in Table I. The frequency range over which the oscillators could be locked by mutual injection was measured to be 12 MHz. Fig. 5 shows the measured and predicted output spectrum for the array under consideration in this paper. Fig. 6

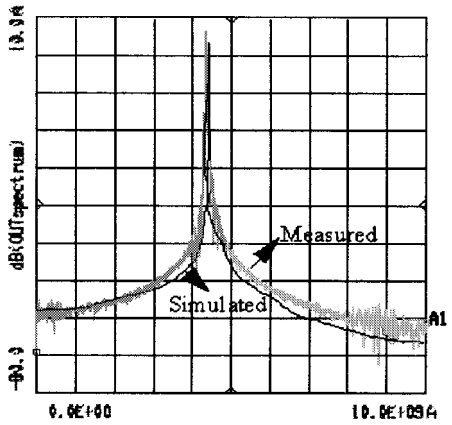

Fig. 5. Output signal from antenna.

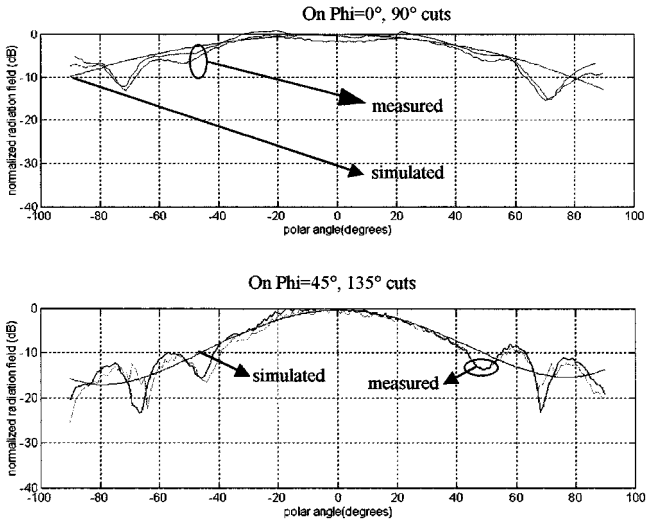

Fig. 6. Simulated and measured antenna far-field radiation patterns on $\phi = 0°$, $45°$, $90°$, and $135°$ cuts ($Vdc1 = 1.20$ V, $Vdc2 = 1.21$ V, $Vdc3 = 1.21$ V, $Vdc4 = 1.22$ V).

shows measured and simulated antenna radiation patterns for various polar pattern cuts when operated in the frequency entrained mode.

Finally, experiments on injection locking of the oscillators were carried out by injecting a signal from a short dipole placed normal to the array at the center of the array network. Due to the monopole-like radiation pattern from this element, it provides a uniform entrainment signal to each element in the array, but does not contribute significantly to the boresight radiation from the

circular patch elements. The estimated injection power into the oscillator group was -6 dBm (the output from each oscillator was set at approximately 4 dBm ($V\text{bias}\approx 1.2$ V). Using this injection-locking scheme, the observed frequency-locking range was increased from 10 MHz using oscillator mutual locking alone to 20 MHz.

VI. Conclusions

An active injection-locked sequentially rotated antenna array has been demonstrated in this paper. Experimental, theoretical, and simulation evidence has been given for its behavior. The antenna utilized four linearly polarized circular microstrip patch-antenna elements with capacitive ring-coupled self-biased MMIC GaAs oscillators as the active sources. As a result of this experiment, it is evident that by using the array suggested in this paper as a basic building block, a multi-MMIC active antenna array could be constructed in order to produce spatial power combining. In addition, for such an array, two-dimensional (2-D) beam-scanning effects could be introduced by detuning individual groups of ring oscillators and/or by frequency pulling a group of ring-coupled oscillators by the use of the dipole injection method introduced above. However, the dynamics of this arrangement are complex, especially when circular polarization is involved, and this aspect is a topic for further study. Such a structure may have potential as a building block in applications such as low-cost spatial power combining for personal communication and radar systems where circular polarization is required.

Acknowledgment

The authors would like thank J. Knox, The Queen's University of Belfast, Belfast, Northern Ireland, and A. Black, The Queen's University of Belfast, Belfast, Northern Ireland, for the fabrication of the antenna array.

References

[1] J. D. Mink, "Quasioptical power combining of solid-state millimeter-wave sources," *IEEE Trans. Microwave Theory Tech.*, vol. MTT-34, pp. 273–279, Feb. 1986.

[2] Y. Qian and T. Itoh, "Progress in active integrated antennas and their applications," *IEEE Trans. Microwave Theory Tech.*, vol. 46, pp. 1891–1900, Nov. 1998.

[3] R. A. York and T. Itoh, "Injection and phase locking techniques for beam control," *IEEE Trans. Microwave Theory Tech.*, vol. 46, pp. 1920–1929, Nov. 1998.

[4] D. E. J. Humphrey, V. F. Fusco, and S. Drew, "Active antenna array behavior," *IEEE Trans. Microwave Theory Tech.*, vol. 43, pp. 1819–1825, Oct. 1995.

[5] K. D. Stephan and W. A. Morgan, "Analysis of injection-locked oscillators for integrated phased arrays," *IEEE Trans. Antennas Propagat.*, vol. AP-35, pp. 771–781, July 1987.

[6] R. Ispir, S. Nogi, and M. Sanagi, "Two-dimensional unilaterally coupled active antenna arrays with wide angle beam scanning capability," in *29th European Microwave Conf. Dig.*, Munich, Germany, 1999, pp. 68–71.

[7] C. J. Wang, C. F. Jou, J. J. Wu, and S. T. Peng, "Radiation characteristics of active frequency-scanning leaky-mode antenna arrays," *IEICE Trans. Electron.*, vol. E82C, no. 7, pp. 1223–1228, 1999.

[8] S. Nogi, S. Lin, and T. Itoh, "Model analysis and stabilization of a spacial power combining array with strongly coupled oscillators," *IEEE Trans. Microwave Theory Tech.*, vol. 41, pp. 1827–1837, Oct. 1993.

[9] D. E. J. Humphrey and V. F. Fusco, "Active antenna array lumped ring configuration," *IEEE Trans. Antennas Propagat.*, vol. 46, pp. 1279–1284, Sept. 1998.

[10] L. Dussopt and J. M. Laheurte, "Coupled oscillator array generating circular polarization," *IEEE Microwave Guided Wave Lett.*, vol. 9, pp. 160–162, Apr. 1999.

[11] J. Birkland and T. Itoh, "A circularly polarized FET oscillator active radiating element," in *IEEE MTT-S Int. Microwave Symp. Dig.*, 1991, pp. 1265–1268.

[12] "F20 process," GEC-Marconi Mater. Technol., Caswell, U.K.

[13] B. Van der Pol, "The nonlinear theory of electrical oscillators," *Proc. IRE*, vol. 22, no. 9, pp. 1051–1086, Sept. 1934.

[14] R. A. York and R. C. Compton, "Measurement and modeling of radiative coupling in oscillator arrays," *IEEE Trans Microwave Theory Tech.*, vol. 41, pp. 438–444, Mar. 1993.

[15] "HP MDS," Hewlett-Packard, Santa Rosa, CA.

[16] "HP high-frequency structure simulator," Hewlett-Packard, Palo Alto, CA.

[17] J. Huang, "A technique for an array to generate circular polarization with linearly polarized elements," *IEEE Trans Antennas Propagat.*, vol. AP-34, pp. 1113–1123, Sept. 1986..

Suidong Yang was born in Chengdu, Sichuan, China, in 1964. He received the B.Sc. degree in applied physics from the National Defence University of Science and Technology, Changsa, Hunan, China, in 1984, the M.Phil. degree in laser technique from South-West Institution of Technical Physics, Chengdu, China, in 1987, and the Ph.D. degree at the Open University, Oxford, U.K., in 1997.

From 1987 to 1991, he was a Research Engineer involved with the study of RF-excited continuous-wave (CW) phase-locked CO_2 laser arrays and pulsed CO_2 lasers at the South-West Institution of Technical Physics. From 1993 to 1997, he was with the Oxford Research Unit, Open University, Oxford, U.K., where he was involved with low-temperature low-pressure inductively coupled RF plasma in the application of semiconductor processing. In May 1997, he joined the High Frequency Electronics Research Group, The Queen's University Belfast, Northern Ireland. His current research interests are waveguide transmission-line discontinuity-modeling, MMIC design, and on-wafer millimeter-wave and semiconductor device-characterization measurement techniques.

Vincent F. Fusco (S'82–M'82–SM'96) received the B.Sc. (first-class honors), Ph.D., and D.Sc. degrees from The Queens University of Belfast, Belfast, Northern Ireland, in 1979, 1982, and 2000, respectively.

He was a Research Engineer involved with short-range radar and radio telemetry systems. He is currently a Professor of high-frequency electronic engineering in the Department of Electrical and Electronic Engineering, The Queen's University of Belfast, where he is Head of the High Frequency Research Group and Associate Dean of Research for Engineering. He has been a consultant to government and international companies. His current research interests include nonlinear microwave circuit design, active antenna design, and concurrent techniques for electromagnetic-field problems. He has authored or co-authored over 240 research papers in these areas and authored *Microwave Circuits, Analysis and Computer Aided Design* (Englewood Cliffs, NJ: Prentice Hall, 1987).

Prof. Fusco is a member of the Institution of Electrical Engineers (IEE) E11, U.K. and various International Scientific Radio Union (URSI) committees. He was the recipient of the 1996 Northern Ireland (NI) Engineering Federation Trophy for exemplary industrially related research.

Denver E. J. Humphrey (S'94–M'96) was born in Ballymena, Northern Ireland, on July 15, 1972. He received the B.Eng. and Ph.D. degrees from The Queen's University of Belfast, Belfast, Northern Ireland, in 1993 and 1996, respectively.

He was with the High Frequency Electronics Research Group, Queen's University. His specific areas of interest are in active antenna arrays and coupled oscillators. He is currently a Design Engineer with TDK Ireland, Belfast, Ireland.